

RADIATION HEAT TRANSFER AT A SURFACE HAVING BOTH SPECULAR AND DIFFUSE REFLECTANCE COMPONENTS

E. M. SPARROW and S. L. LIN

Heat Transfer Laboratory, Department of Mechanical Engineering, University of Minnesota, Minneapolis, Minnesota

(Received 19 October 1964 and in revised form 26 November 1964)

Abstract—A method of analysis has been devised for determining the radiant interchange among surfaces, each of which may have both specular and diffuse reflectance components. The formulation uses and generalizes the exchange factor concept (which was initially devised for specularly-reflecting surfaces) and the radiosity concept (which was initially devised for diffusely-reflecting surfaces). Various forms of the analytical method are presented that are suitable either for overall engineering-type computations or for more detailed local investigations. Specific analytical and numerical consideration is given to radiant interchange in cylindrical and conical cavities and to radiant transport through a circular tube. Results are presented for various subdivisions of the surface reflectance into specular and diffuse components. In general, it is found that the radiant efflux from a cavity increases as the specular component becomes a larger fraction of the surface reflectance. A similar statement applies for the transmission of radiant energy through a tube.

NOMENCLATURE

A ,	surface area;
B ,	radiosity;
E , dE ,	exchange factor;
F , dF ,	angle factor;
H ,	incident energy/time-area;
L ,	length or depth;
Q ,	overall heat-transfer rate;
q ,	local heat-transfer rate/area;
R ,	radius;
r ,	position co-ordinate;
x ,	axial co-ordinate;
T ,	absolute temperature;
ϵ ,	surface emittance;
ϵ_a ,	apparent emittance of cavity;
θ ,	dimensionless temperature, equation (23a);
ξ ,	dummy variable;
ρ ,	hemispherical reflectance;
ρ^s ,	specular reflectance component;
ρ^d ,	diffuse reflectance component;
σ ,	Stefan-Boltzmann constant;
φ ,	cone half-opening angle.

INTRODUCTION

IN COMPUTING the exchange of thermal radiation between surfaces, it has been customary to formulate the equations of radiant interchange

under the assumption that the participating surfaces are perfectly diffuse reflectors. Recently, in recognition of the fact that many real surfaces do possess a significant specular component, there have appeared several papers [1-5] dealing with radiant interchange among surfaces that are perfectly specular reflectors. Consideration has also been extended to enclosures in which some of the surfaces are specularly-reflecting and others are diffusely-reflecting [2, 3].

The present investigation is concerned with surfaces that possess both specular and diffuse reflectance components,† as is the case with actual engineering surfaces. As a first approximation, it is reasonable to represent the hemispherical reflectance ρ as being subdivided into diffuse and specular components ρ^d and ρ^s respectively.

$$\rho = \rho^d + \rho^s \quad (1)$$

Indeed, such a representation has already been suggested by Seban in an incisive discussion appended to reference 2. Moreover, magnitudes of ρ^s and ρ for metallic surfaces‡ of various roughness have been reported in reference 6.

† Added in proof: Contemporaneous studies are presented in references 11 and 12.

‡ Specifically nickel.

In the development that follows, the aforementioned model of the reflection process is employed in formulating the equations of radiant interchange. The formulation uses concepts that have evolved [3, 5] subsequent to the Seban suggestion. Furthermore, specific consideration is given here to radiant interchange in the long cylindrical cavity, in the conical cavity, and in a circular tube connecting isothermal environments. The governing integral equations for these configurations are solved for various subdivisions of the reflectance into diffuse and specular components. Numerical results are presented which display the effect of such subdivisions.

THE EXCHANGE FACTOR

In problems of radiant interchange involving specularly-reflecting, diffusely-emitting surfaces, it has been highly convenient [3, 5] to make use of the exchange factor concept. It will be demonstrated later that exchange factors for purely specularly-reflecting surfaces can be employed directly in the equations of radiant interchange for surfaces having both diffuse and specular reflectance components. Before proceeding to this generalization, it is useful to review and illuminate the exchange factor concept.

As introduced in reference 3 and elucidated in reference 5, the exchange factor represents the fraction of the diffusely-emitted radiation that leaves one area element and arrives at a second area element both directly and by all possible *specular* inter-reflections. The exchange factor $dE_{dA_i-dA_j}$ relating to radiation leaving dA_i and arriving at dA_j has the general form

$$dE_{dA_i-dA_j} = f_0 + \rho_{11}^s f_1 + \rho_{12}^s \rho_{22}^s f_2 + \rho_{13}^s \rho_{23}^s \rho_{33}^s f_3 + \dots \quad (2)$$

The first term, f_0 , denotes the direct transport between dA_i and dA_j ; therefore, f_0 coincides with the diffuse angle factor $dF_{dA_i-dA_j}$. The second term, $\rho_{11}^s f_1$, corresponds to radiant transport between dA_i and dA_j with one intervening specular reflection. The third term, $\rho_{12}^s \rho_{22}^s f_2$, corresponds to transport with two intervening specular reflections, and so forth. The quantity f_1 is the diffuse angle factor

between dA_i and an intervening element dA_{11} whose size and orientation are determined by the following condition: namely, that radiant energy incident on dA_{11} from dA_i be specularly reflected to dA_j without further intervening specular reflections. The specular reflectance at dA_{11} is denoted by ρ_{11}^s .

The quantity f_2 is the diffuse angle factor between dA_i and an element dA_{12} whose size and orientation are constrained as follows: that radiant energy arriving at dA_{12} from dA_i be specularly reflected to dA_j with one additional intervening specular reflection. The specular reflectance at dA_{12} is ρ_{12}^s , and ρ_{22}^s is the specular reflectance at an element dA_{22} at which the aforementioned intervening specular surface contact occurs. The quantity f_3 and the reflectances ρ_{13}^s , ρ_{23}^s , and ρ_{33}^s are similarly interpreted, and so forth.

It may be noted that in some situations, there may be more than one path by which radiation may pass from dA_i to dA_j with one intervening specular reflection. Correspondingly, the term $\rho_{11}^s f_1$ in equation (2) would be evaluated for each such path. A similar statement applies to all the terms of the series.

Equation (2) represents the exchange factor for interchange between two infinitesimal elements dA_i and dA_j . Similar expressions apply for the exchange factors $E_{dA_i-A_j}$ and $E_{A_i-A_j}$; the only change is that the f quantities now represent finite angle factors rather than infinitesimal angle factors as before.

For cases in which the specularly-reflecting surfaces are plane, exchange factors are readily determined by employing the image method from references 1 and 2. When the specularly-reflecting surfaces are nonplanar, then the image method cannot be applied directly. Exchange factors corresponding to interchange within a specularly-reflecting, diffusely-emitting cylindrical tube have been derived in reference 3 with the aid of physical reasoning. For more general curved-surface configurations, a formal method of analysis has been devised [5] for determining the exchange factors, and this has been applied to the conical cavity and to the cylindrical cavity of finite depth. It is not the present purpose to dwell at length on the details of determining exchange factors inasmuch as

the best available methods are suitably documented in the aforementioned references. However, before concluding this section, it may be well to state the reciprocity relationships

$$dA_i dE_{dA_i-dA_j} = dA_j dE_{dA_j-dA_i};$$

$$dA_i E_{dA_i-A_j} = A_j dE_{A_j-dA_i} \quad (3a)$$

$$A_i E_{A_i-A_j} = A_j E_{A_j-A_i} \quad (3b)$$

THE EQUATIONS OF RADIANT INTERCHANGE FOR SPECULARLY-DIFFUSELY REFLECTING SURFACES

The equations of radiant interchange will now be formulated for the condition where the participating surfaces possess both specular and diffuse reflectance components.

The starting point of the derivation is a reconsideration of the radiosity concept. For a diffusely-emitting and diffusely-reflecting surface, the radiosity is defined as the radiant energy leaving a surface per unit time and unit area. Moreover, for such surfaces, it is evident that the radiosity is the sum of the emitted radiation and the reflected radiation.

Now, consider a surface which possesses both specular and diffuse reflectance components. Let H represent the radiant flux incident on a surface per unit time and unit area. Then, for a diffusely-emitting surface with a diffuse reflectance component ρ^d , an appropriate definition of the radiosity B is

$$B = \epsilon \sigma T^4 + \rho^d H \quad (4)$$

It is evident that B represents the *diffusely-distributed* radiant flux leaving a surface element per unit time and unit area.

Although the exchange factor was originally formulated to describe the fraction of the *diffusely-emitted* radiant energy passing from an emitter to a receiver, it applies equally well for any diffusely-distributed radiant flux leaving a surface. Thus, for example, if $B_i dA_i$ is the flux of diffuse radiation leaving the element dA_i , then the amount

$$B_i dA_i dE_{dA_i-dA_j}$$

will arrive at the element dA_j , both directly and by all possible specular inter-reflections. With

these ideas in hand, consideration may now be given to the equations of radiant interchange.

Graybody enclosure theory

Attention will first be directed to generalizing the engineering-type computation procedure that deals with a system made up of N finite surfaces. The basic postulates of such computations are as follows: (a) each surface is isothermal, (b) each surface is a graybody, (c) each surface is a diffuse emitter, (d) each surface is a diffuse reflector, (e) the radiosity is uniformly distributed across each surface. The present formulation removes postulate (d) and employs instead a reflectance model described by equation (1).

The first step in the analysis is to derive an expression for the radiant flux H that is incident per unit time and unit area at a typical surface i (area A_i) in the enclosure. Consideration may first be given to the radiation arriving at surface i from another surface j . Now, the radiant energy leaving surface j is composed of a diffusely-distributed portion $B_j A_j$ plus a specularly-reflected portion. The specularly-reflected radiation is fully included in the exchange factors. Of the diffusely-distributed radiation leaving surface j , a quantity $B_j A_j E_{j-i}$ arrives at surface i both directly and by all possible intervening specular inter-reflections. Moreover, by applying the reciprocity relation (3b), the foregoing energy quantity is equal to $B_j A_i E_{i-j}$. Such contributions arrive at A_i from all of the surfaces of the enclosure and therefore H_i is represented by the summation

$$H_i = \sum_{j=1}^N B_j E_{i-j} \quad (5)$$

It should be emphasized that equation (5) contains the contributions of both specularly and diffusely reflected radiation, the former being accounted for by the exchange factors.

In general, there are two thermal boundary conditions that may be of interest: (a) prescribed surface temperature, (b) prescribed surface heat-transfer rate. A special case of the latter is the adiabatic or no-flux surface. Suppose that among the N surfaces of the enclosure, those that are designated as 1, 2, ..., N_1 have prescribed

temperatures while those designated as $(N_1 + 1)$, $(N_1 + 2)$, \dots , N have prescribed heat flux.

For the surfaces with prescribed temperature, one may eliminate H between equations (4) and (5) and obtain

$$B_i = \epsilon_i \sigma T_i^4 + \rho_i^a \sum_{j=1}^N B_j E_{i-j}, \quad 1 \leq i \leq N_1 \quad (6)$$

On the other hand, a somewhat different form of the radiant flux balance is appropriate for those surfaces having prescribed heat flux. First of all, it may be noted that the net rate of heat transfer Q_i at a surface i is the difference between the radiation leaving the surface and that which is incident on the surface. The rate at which radiation leaves the surface is

$$(B_i + \rho_i^s H_i) A_i,$$

while the rate of incident radiation is $H_i A_i$. Upon differencing these quantities and introducing H_i from equation (5), one has

$$B_i = Q_i/A_i + (1 - \rho_i^s) \sum_{j=1}^N B_j E_{i-j}, \quad (N_1 + 1) \leq i \leq N \quad (7)$$

Upon inspecting equations (6) and (7), it is seen that there are a total of N unknowns: $B_1, B_2, B_3, \dots, B_N$; correspondingly, there are N linear algebraic equations. The T_i^4 are prescribed constants for $1 \leq i \leq N_1$; while the Q_i are prescribed for $(N_1 + 1) \leq i \leq N$. The radiation properties for each surface are related by

$$\rho = 1 - \epsilon = \rho^a + \rho^s \quad (8)$$

where the graybody condition has been employed.

Once the radiosities have been determined from the solution of equations (6) and (7), then the surface heat flux or surface temperature, whichever is unknown, can be computed directly. For those surfaces wherein the temperature is prescribed, the heat-transfer rate is given by

$$\frac{Q_i}{A_i} = \frac{\epsilon_i}{\rho_i^a} [(\rho_i^a + \epsilon_i) \sigma T_i^4 - B_i], \quad 1 \leq i \leq N_1 \quad (9)$$

In the event that one or more of the surfaces having prescribed temperature are purely

specularly-reflecting ($\rho^a = 0$), then equation (9) is replaced by

$$Q_i/A_i = \epsilon_i [\sigma T_i^4 - \sum_{j=1}^N B_j E_{i-j}] \quad (10)$$

On the other hand, for those surfaces at which the heat flux is prescribed, the corresponding temperature is

$$\sigma T_i^4 = \frac{\epsilon_i B_i + \rho_i^a (Q_i/A_i)}{\epsilon_i (1 - \rho_i^s)}, \quad (N_1 + 1) \leq i \leq N \quad (11)$$

Integral equation formulation

Consideration is once again given to an enclosure consisting of N finite surfaces, except that now the radiosity, temperature, and heat flux vary with local position across each surface. A co-ordinate system may be established such that the position vector designating points on surface i is \mathbf{r}_i , the position vector designating points on surface j is \mathbf{r}_j , and so forth.

The equations of radiant interchange are derived in a manner similar to that of the preceding section. For those surfaces $1 \leq i \leq N_1$ for which the temperature is prescribed, the radiant-flux equations are

$$B_i(\mathbf{r}_i) = \epsilon_i \sigma T_i^4(\mathbf{r}_i) + \rho_i^a \sum_{j=1}^N \int_{A_j} B_j(\mathbf{r}_j) dE_{dA_i-dA_j} \quad (12)$$

Furthermore, for those surfaces

$$(N_1 + 1) \leq i \leq N$$

at which the heat-transfer rate is prescribed

$$B_i(\mathbf{r}_i) = q_i(\mathbf{r}_i) + (1 - \rho_i^s) \sum_{j=1}^N \int_{A_j} B_j(\mathbf{r}_j) dE_{dA_i-dA_j} \quad (13)$$

in which q is the local heat-transfer rate per unit time and unit area. Equations (12) and (13) contain N unknown functions $B_1(\mathbf{r}_1), B_2(\mathbf{r}_2), \dots, B_N(\mathbf{r}_N)$. Correspondingly, there are N linear integral equations. These equations are of the same form as the integral equations of radiant interchange for purely diffusely-reflecting surfaces.

Once the solutions for the $B_i(\mathbf{r}_i)$ have been found, then the corresponding distributions of T_i and q_i follow as

$$q_i(\mathbf{r}_i) = (\epsilon_i/\rho_i^d) [(\rho_i^d + \epsilon_i) \sigma T_i^4(\mathbf{r}_i) - B_i(\mathbf{r}_i)], \quad 1 \leq i \leq N_1 \quad (14)$$

$$\sigma T_i^4(\mathbf{r}_i) = \frac{\epsilon_i B_i(\mathbf{r}_i) + \rho_i^d q_i(\mathbf{r}_i)}{\epsilon_i (1 - \rho_i^d)}, \quad (N_1 + 1) \leq i \leq N \quad (15)$$

In the former case, if $\rho^d = 0$, then equation (14) is replaced by

$$q_i(\mathbf{r}_i) = \epsilon_i [\sigma T_i^4(\mathbf{r}_i) - \sum_{j=1}^N \int_{A_j} B_j(\mathbf{r}_j) dE_{\alpha A_i - \alpha A_j}] \quad (14a)$$

THE GOVERNING EQUATIONS FOR SPECIFIC CAVITIES AND PASSAGES

Specific study will be made here of radiant interchange in the following configurations: the circular cylindrical cavity, the conical cavity, and the circular tube that connects two isothermal environments. The equations of radiant interchange appropriate to these problems will now be stated. Results are presented in the final section of the paper.

Cylindrical cavity

Consider a circular cylindrical cavity of radius R and depth L . The cavity wall has a uniform temperature T_w . Radiation emitted at the walls is diffusely-distributed, while there are both specular and diffuse reflectance components. Initially, it will be assumed that there is negligible radiant energy entering the cavity through its opening; later, the results will be generalized to account for such incoming radiation. The cavity emission problem just described has been solved for the limiting case of purely diffuse reflectance in a number of investigations, the most recent being reference 7. Very recently, results for the other limit of purely specular reflectance have been published [5].

In the present investigation, the analysis will be restricted to cavities whose depth $L \gg R$. This assumption is invoked to reduce the number of independent parameters and thereby to bring the subsequent numerical computations within reasonable bounds. There is no conceptual difficulty in solving the cavity of finite depth.

Let the axial distance from the cavity opening

be denoted by x . Then, by specializing equation (12), one finds

$$B(x) = \epsilon \sigma T_w^4 + \rho^d \int_{\xi=0}^{\infty} B(\xi) dE_{x-\xi} \quad (16)$$

in which ξ is a dummy variable. The exchange factor $dE_{x-\xi}$ is available in references 3 and 5. In the limit as $x \rightarrow \infty$, it is readily shown that $B \rightarrow (\epsilon + \rho^d) \sigma T_w^4$. When the dimensionless variables $B/\sigma T_w^4$ and x/R are introduced into equation (16), it is seen that the three radiation properties ϵ , ρ^d , and ρ^s appear as parameters (the latter is included in dE). However, in light of equation (8), only two of these three properties are independent parameters that need be prescribed.

The solution of equation (16) was obtained numerically by an iterative technique. In practice, the upper limit on the integral was taken as a finite value ξ^* selected so that B approached very closely to the aforementioned limiting value.

The distribution of the local heat flux as a function of axial position is readily evaluated from equation (14) once the solutions for B have been obtained. In turn, the rate Q at which radiant energy streams out of the cavity opening is found by integrating the local q values, thus

$$Q = \int_0^{\infty} q 2\pi R dx \quad (17)$$

The overall heat-transfer results for a cavity can be expressed in terms of an apparent emittance ϵ_a which is the ratio of the actual heat flux Q to that which is radiated by a black cavity, thus

$$\epsilon_a = Q/\pi R^2 \sigma T_w^4 = 2 \int_0^{\infty} (q/\sigma T_w^4) d(x/R) \quad (17a)$$

The analysis will now be extended to include radiant energy entering the cavity from the external environment. Suppose that the incoming radiation is uniformly and diffusely distributed across the cavity opening and that the magnitude of such radiation is expressed as an equivalent blackbody temperature T_{∞} . Then, the preceding analysis goes through as before, except that wherever T_w^4 formerly appeared, one now writes $T_w^4 - T_{\infty}^4$.

Conical cavity

The next configuration to be studied is a conical cavity having an isothermal wall at temperature T_w . The cone half-opening angle is φ , while the slant-height is L ; x measures distances along the slant height from the cone vertex. Results for the limiting cases of purely diffuse reflection and purely specular reflection are respectively available in references 8 and 5.

For the situation in which the incoming radiation is negligible, the specialization of equation (12) leads to

$$B(x) = \epsilon\sigma T_w^4 + \rho^d \int_{\xi=0}^L B(\xi) dE_{x-\xi} \quad (18)$$

in which ξ is once again a dummy variable. The exchange factor appearing under the integral sign has been derived in reference 5. If equation (18) is rephrased using dimensionless variables $B/\sigma T_w^4$ and x/L , it is found that four parameters appear: the radiation properties ϵ , ρ^d , and ρ^s , and the half-opening angle φ (the last two of these are contained in dE). In view of the relationship between the properties, equation (8), it is evident that solutions of the integral equation (18) will depend on the specification of three independent parameters.

Equation (18) was solved numerically by an iterative procedure and corresponding local heat flux values were deduced from equation (14). In turn, the overall heat-transfer rate Q was computed by integration of the local heat flux

$$Q = \int_0^L q \, 2\pi x \sin \varphi \, dx \quad (19)$$

In terms of the apparent emittance ϵ_a , equation (19) becomes

$$\epsilon_a = \frac{Q}{\pi L^2 \sin^2 \varphi \sigma T_w^4} = \frac{2}{\sin \varphi} \int_0^1 \frac{q}{\sigma T_w^4} \frac{x}{L} d\left(\frac{x}{L}\right) \quad (19a)$$

The foregoing analysis can be generalized to include radiant energy entering the cavity from the external environment by incorporating modifications identical to those outlined for the circular cylindrical cavity.

Transmission of radiant energy through a tube

Consider next a circular tube of length L and radius R that connects two isothermal environments. The blackbody temperature of the environment adjacent to the left-hand end of the tube is T_1 , while the blackbody temperature of the environment adjacent to the right-hand end of the tube is T_2 . The axial co-ordinate x measures distances from the left-hand end. It is desired to find the radiant energy that is transported through the tube under the condition that the tube wall is locally adiabatic, i.e. $q = 0$. Results for the limiting cases of purely diffuse reflection and purely specular reflection have been published respectively in references 3 and 9 and in reference 3.

In carrying out the analysis, it is advantageous to note that the problem is linear in the fourth power of the temperature. Thus, without loss of generality, one can conceive of the tube as having an environment at zero temperature at its right-hand end, an environment at temperature $T_1^4 - T_2^4$ at its left-hand end, and a local wall temperature $T_w^4(x) - T_2^4$ at x .

The governing integral equation is most easily derived by specializing equation (13). Upon applying this equation at a typical point x on the tube wall and setting $q = 0$, one gets

$$B(x) = (1 - \rho^s) [B_1 E_{x-1} + B_2 E_{x-2} + \int_{\xi=0}^L B(\xi) dE_{x-\xi}] \quad (20)$$

The first two terms in the brackets correspond to radiant energy arriving at location x from the environments. Since the latter are black radiators, one can write

$$B_1 = \sigma (T_1^4 - T_2^4), \quad B_2 = 0 \quad (21)$$

Moreover, by applying equation (15) with $q = 0$, there follows

$$B(x) = (1 - \rho^s) \sigma [T_w^4(x) - T_2^4], \\ B(\xi) = (1 - \rho^s) [T_w^4(\xi) - T_2^4] \quad (22)$$

Upon introducing these into equation (20), there is obtained

$$\theta(x) = E_{x-1} + (1 - \rho^s) \int_{\xi=0}^L \theta(\xi) dE_{x-\xi} \quad (23)$$

wherein

$$\theta = (T_w^4 - T_2^4)/(T_1^4 - T_2^4) \quad (23a)$$

Equation (23) is the governing integral equation for the axial distribution of the tube wall temperature.

The net rate of energy throughflow from environment 1 to environment 2, denoted by Q , is the difference between the radiant energy streaming into and out of the tube opening at 1, thus

$$Q/\pi R^2(T_1^4 - T_2^4) = 1 - (1 - \rho^s) \int_{x=0}^L \theta(x) dE_{1-x} \quad (24)$$

Upon inspecting equations (23) and (24) and noting that dE contains ρ^s (but no other radiation property), it is seen that the temperature distribution and the energy transport depend on a single radiation property, ρ^s . In other words, the results are determined once and for all as soon as ρ^s is specified, regardless of the value of the diffuse component ρ^d .

In addition to ρ^s , the solutions also depend parametrically on the tube aspect ratio L/R . The exchange factors appearing in equations (23) and (24) are available in references 3 and 5. Numerical solutions of the integral equation (23) were carried out by an iteration procedure.

RESULTS

Cylindrical cavity

Results for the overall and the local heat transfer for the cylindrical cavity of infinite

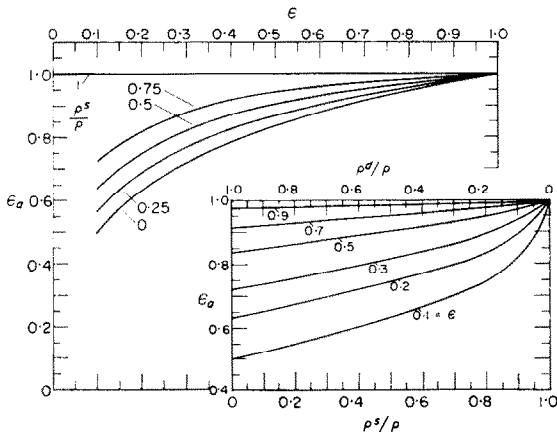


FIG. 1. Overall heat-transfer results for deep cylindrical cavities.

depth are respectively presented in Figs. 1 and 2. Figure 1 consists of two parts. The upper portion is a plot of the apparent emittance of the cavity ϵ_a [see equation (17a) for definition] as a function of the emittance ϵ of the cavity wall. Curves are shown for cases in which the reflectance is purely specular, $\rho^s/\rho = 1$; purely diffuse, $\rho^s/\rho = 0$; or is partly specular and partly diffuse, $\rho^s/\rho = 0.25, 0.5$, and 0.75 . The lower portion of the figure is a cross plot of the information appearing in the upper portion. It shows, for various fixed values of surface emittance, the variation of ϵ_a as the reflectance ranges from purely diffuse to purely specular.

By inspection of Fig. 1, it is seen that for any given surface emittance, the radiant emission of the cavity is greatest when the wall is specularly reflecting and least when the wall is diffusely reflecting. Cavities having surface reflectances that are partly specular and partly diffuse lie intermediate between the aforementioned limits. The increase of ϵ_a with increasing ρ^s/ρ is most marked for surfaces characterized by small values of the emittance ϵ . Moreover, for such surfaces, the sharpest increases in ϵ_a occur as ρ^s/ρ approaches unity.

Further study reveals that in all cases, the apparent emittance ϵ_a exceeds the surface emittance ϵ ; this is especially marked for surfaces of lower emittance and is further accentuated as the reflectance becomes more specular.

Consideration may now be given to the local heat-transfer results that are exhibited in Figs. 2(a), 2(b), and 2(c). These figures correspond

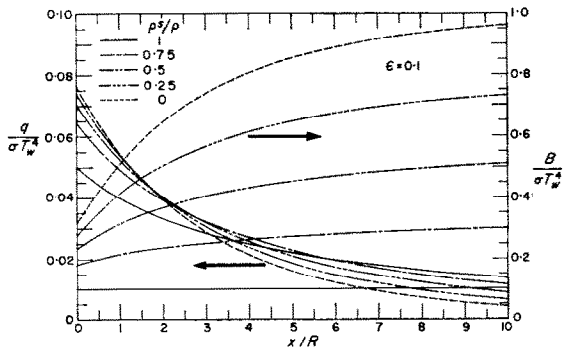


FIG. 2(a). Local heat-transfer and radiosity distributions for deep cylindrical cavities, $\epsilon = 0.1$.

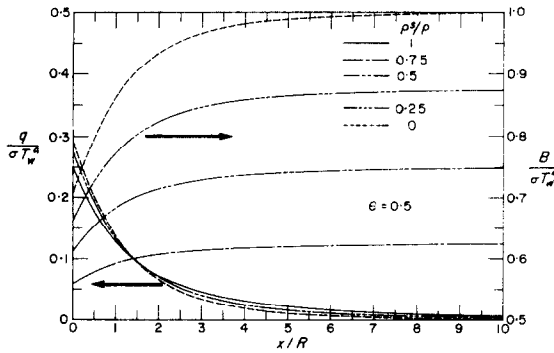


FIG. 2(b). Local heat-transfer and radiosity distributions for deep cylindrical cavities, $\epsilon = 0.5$.

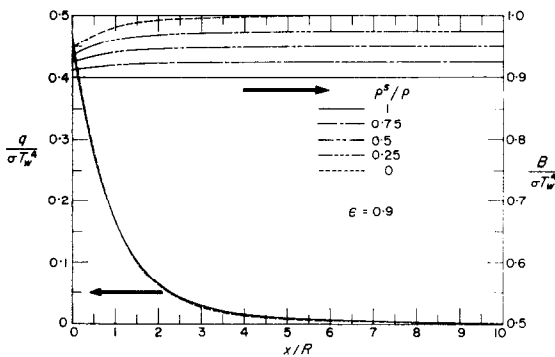


FIG. 2(c). Local heat-transfer and radiosity distributions for deep cylindrical cavities, $\epsilon = 0.9$.

respectively to surface emittances ϵ of 0.1, 0.5, and 0.9. Results for other values of ϵ are available in reference 10, but these must be omitted here due to space limitations. Each of the aforementioned figures contains two sets of curves. Those sloping downward to the right represent the local heat flux and are referred to the left-hand ordinate, while those sloping upward to the right represent the local radiosity and are referred to the right-hand ordinate. The abscissa is the axial distance from the cavity opening.

The figures show that in the neighborhood of the cavity opening, the local heat flux is largest when the cavity wall is a pure diffuse reflector and decreases as the specular component increases. On the other hand, in the interior of the cavity, an opposite trend exists; that is, the local heat flux is largest at a specularly-reflecting surface and is least at a diffusely-reflecting surface. These trends are most strongly in

evidence at lower values of the surface emittance ϵ .

As to the radiosity, the highest values at any fixed emittance ϵ correspond to the diffusely-reflecting surface; this applies at any axial location.

Conical cavity

The governing integral equation (18) for the conical cavity has been solved for parametric values of $\epsilon (= 1 - \rho)$, of ρ^s/ρ , and of the half-opening angle φ . The corresponding local and overall heat-flux results were computed from equations (14) and (19a). This information is presented in Figs. 3 and 4, respectively for the overall and local heat fluxes.

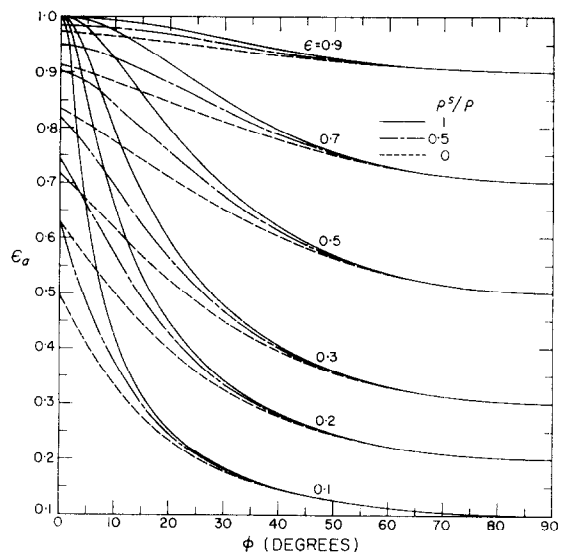


FIG. 3. Overall heat-transfer results for conical cavities.

Attention may first be directed to Fig. 3, wherein there is plotted the apparent emittance of the cavity ϵ_a as a function of the cone half-opening angle φ . The curves are labelled according to the surface emittance ϵ . Furthermore, for each ϵ , results are shown for reflectances that are purely specular, $\rho^s/\rho = 1$; purely diffuse, $\rho^s/\rho = 0$; and for half specular and half diffuse, $\rho^s/\rho = 0.5$.

Inspection of the figure indicates that the apparent emittance increases monotonically with increasing ρ^s/ρ ; thus, at a fixed surface emittance ϵ , the specularly-reflecting cavity

radiates most energy and the diffusely-reflecting cavity least. The curves corresponding to $\rho^s/\rho = 0.5$ do not necessarily lie half way between those for purely specular and purely diffuse reflectance, although this behavior is nearly achieved when the surface emittance is high. At lower values of surface emittance, the curves for $\rho^s/\rho = 0.5$ lie closer to those for diffuse reflectance when φ is small and closer to those for specular reflectance when φ takes on intermediate values. For still larger cone opening angles, all results approach the limit $\epsilon_a = \epsilon$. In general, it can be stated that the apparent emittance becomes independent of the directional distribution of the reflectance for $\varphi \geq 40^\circ$.

A graphical presentation of the axial distribution of the local heat flux is made in Figs. 4(a), 4(b), and 4(c), respectively for $\epsilon = 0.1, 0.5$, and 0.9 . This information is given as a function of x/L , the fractional distance along the slant

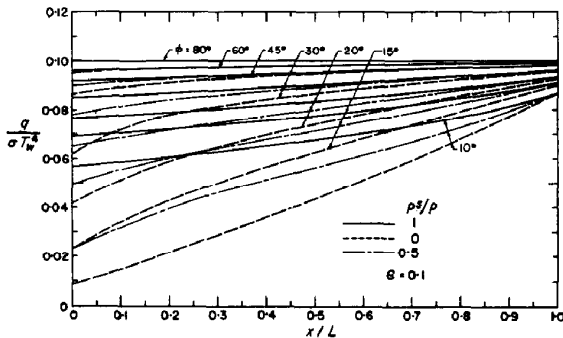


FIG. 4(a). Local heat-transfer distributions for conical cavities, $\epsilon = 0.1$.

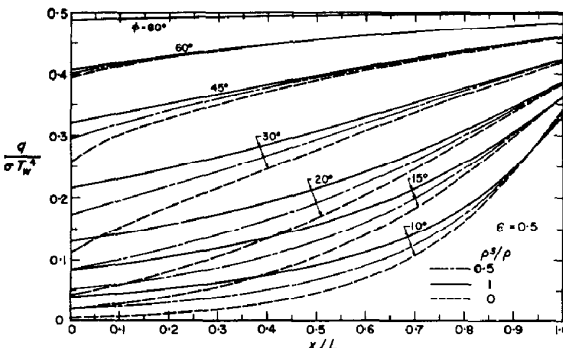


FIG. 4(b). Local heat-transfer distributions for conical cavities, $\epsilon = 0.5$.

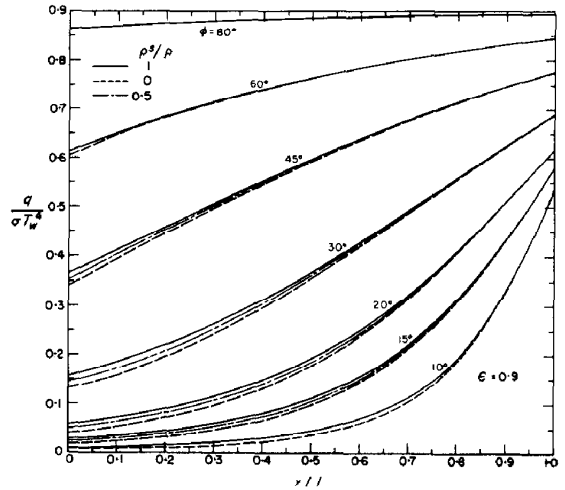


FIG. 4(c). Local heat-transfer distributions for conical cavities, $\epsilon = 0.9$.

height ($x = 0$ is at the cone apex). On each figure, results are shown for several cone half-opening angles between 10° and 80° . Moreover, for each opening angle, curves are plotted for three reflectance conditions, $\rho^s/\rho = 1, 0.5$, and 0 .

In general, for any fixed ϵ , the local heat flux at any position on the cavity wall increases monotonically with ρ^s/ρ . The results are particularly sensitive to ρ^s/ρ at locations nearer the cone apex and are quite insensitive to ρ^s/ρ at locations near the cavity opening. Moreover, cones having small opening angles are much more sensitive to ρ^s/ρ than are cones with large opening angles. Finally, it may be noted that cavities with low surface emittance are also more sensitive to ρ^s/ρ than are cavities with highly emissive walls.

Radiation transport through a circular tube

Solutions of the governing integral equation (23) have been carried out for ρ^s ranging from 0 to 1.0 and for L/R ranging from 1 to 40. Each of these solutions is, in itself, the axial distribution of the adiabatic wall temperature corresponding to the prescribed values of the parameters. The presentation of this information is quite space consuming and is therefore omitted here; however, a complete set of graphs is available in the thesis [10] from which this paper is drawn.

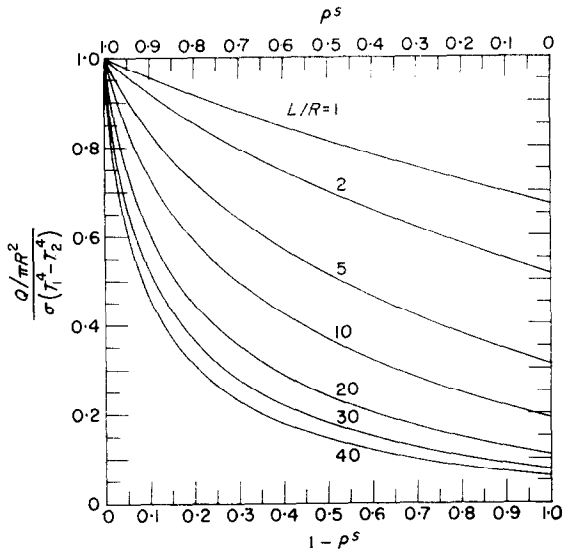


FIG. 5. Transport of radiant energy through a circular tube.

The radiant energy Q transmitted through the tube has been evaluated from equation (24) and is displayed in Fig. 5. The abscissa of the figure is the specular reflectance component ρ^s , and the curves are labelled with the tube aspect ratio. From the figure, it is seen that for a fixed tube geometry, the radiant transmission decreases steadily as the specular reflectance decreases. The results for tubes that are relatively long are particularly sensitive to ρ^s , especially at larger values of ρ^s where the curves are steep. In general, for given thermal conditions, the radiant transmission through short tubes is greater than that through long tubes, regardless of the value of ρ^s .

It is interesting to observe that the radiant transport through a tube having both specular and diffuse reflectance components is identical to the transmission through a purely specularly-reflecting tube, provided that both tubes have equal values of ρ^s . This characteristic permits

comparison of the present results with those of reference 3, the latter having been derived for the specular case. For those conditions where comparisons are possible, there appears to be satisfactory agreement between the two sets of results.

REFERENCES

1. E. R. G. ECKERT and E. M. SPARROW, Radiation heat exchange between surfaces with specular reflection, *Int. J. Heat Mass Transfer* **3**, 42-54 (1961).
2. E. M. SPARROW, E. R. G. ECKERT and V. K. JONSSON, An enclosure theory for radiative exchange between specularly and diffusely reflecting surfaces, *J. Heat Transfer* **C84**, 294-300 (1962).
3. M. PERLMUTTER and R. SIEGEL, Effect of specularly-reflecting gray surfaces on thermal radiation through a tube and from its heated wall, *J. Heat Transfer* **C85**, 55-62 (1963).
4. R. P. BOBCO, Radiation heat transfer in semigray enclosures with specularly and diffusely reflecting surfaces, *J. Heat Transfer* **C86**, 123-130 (1964).
5. S. H. LIN and E. M. SPARROW, Radiant interchange among curved specularly reflecting surfaces; application to cylindrical and conical cavities. ASME Paper No. 64-WA/HT-5. To be published in *J. Heat Transfer*.
6. R. C. BIRKEBAK, E. M. SPARROW and E. R. G. ECKERT, Effect of surface roughness on the total hemispherical and specular reflectance of metallic surfaces, *J. Heat Transfer* **C86**, 193-199 (1964).
7. E. M. SPARROW, L. U. ALBERS and E. R. G. ECKERT, Thermal radiation characteristics of cylindrical enclosures, *J. Heat Transfer* **C84**, 73-81 (1962).
8. E. M. SPARROW and V. K. JONSSON, Radiant emission characteristics of diffuse conical cavities, *J. Opt. Soc. Amer.* **53**, 816-821 (1963).
9. E. M. SPARROW and V. K. JONSSON, The transport of radiant energy through tapered tubes or tapered gaps, *J. Heat Transfer* **C86**, 132 (1964).
10. S. H. LIN, Radiant interchange in cavities and passages with specularly and diffusely reflecting surfaces. Ph.D. Thesis, Department of Mechanical Engineering, University of Minnesota (March 1964).
11. H. C. HOTTEL and A. F. SAROFIN, Radiation exchange among nonideal surfaces, in *Developments in Heat Transfer*, W. A. ROHSENOW (editor), M.I.T. Press, Cambridge, Massachusetts (1964).
12. J. T. BEVANS and D. K. EDWARDS, Radiation exchange in an enclosure with directional wall properties, ASME Paper No. 64-WA/HT-52 (1964).

Résumé—Une méthode d'analyse a été obtenue pour déterminer l'échange par rayonnement entre des surfaces, chacune d'elles pouvant avoir à la fois des composantes de réflexion spéculaire et diffuse. La formulation emploie et généralise le concept du facteur d'échange (qui a été initialement imaginé pour des surfaces à réflexion spéculaire) et le concept de la radiosité (qui a été initialement imaginé pour des surfaces à réflexion diffuse). Des formes variées de la méthode analytique sont présentées qui conviennent soit pour des calculs globaux intéressant l'ingénieur ou pour des recherches locales

plus détaillées. On a considéré spécifiquement d'une façon analytique et numérique l'échange par rayonnement dans des cavités cylindriques et coniques et le transport par rayonnement à travers un tube circulaire. Des résultats sont présentés pour diverses subdivisions du rayonnement réfléchi par la surface en composantes spéculaire et diffuse. En général, on trouve que le rayonnement sortant d'une cavité croît lorsque la composante spéculaire devient une fraction plus grande du rayonnement réfléchi de la surface. Une conclusion semblable se rapport à la transmission du rayonnement à travers un tube.

Zusammenfassung—Zur Bestimmung des Strahlungsaustausches zwischen Oberflächen, von denen jede sowohl eine spiegelnde wie auch eine diffuse Komponente des Reflexionsvermögens hat, wurde eine Methode zum Analysieren aufgestellt. Die Formulierung verwendet und verallgemeinert das Austauschfaktorkonzept (das ursprünglich für spiegelnd reflektierende Oberflächen aufgestellt wurde) und das Strahlungskonzept (das ursprünglich für diffus-reflektierende Oberflächen aufgestellt wurde).

Es werden verschiedene Formen von analytischen Methoden angeführt, die entweder für Pauschalberechnungen des Ingenieurs oder für detaillierte örtliche Untersuchungen geeignet sind. Besondere analytische und numerische Berücksichtigung fand der Strahlungsaustausch in zylindrischen und konischen Vertiefungen und der Strahlungstransport durch ein Kreisrohr. Für verschiedene Unterteilungen des Oberflächenreflexionsfaktors in spiegelnde und diffuse Komponenten werden Ergebnisse angegeben. Allgemein findet man, dass die Strahlungsdichte aus einer Vertiefung zunimmt, wenn die spiegelnde Komponente als grösserer Bruchteil des Oberflächenreflexionsvermögens auftritt. Eine ähnliche Feststellung lässt sich für die Übertragung der Strahlungsenergie durch ein Rohr machen.

Аннотация—Разработана методика анализа для определения лучистого обмена между поверхностями, каждая из которой может обладать как зеркальной, так и диффузионной компонентами отражательной способности. Формулировка использует и обобщает понятие обменного коэффициента (который первоначально был введен для диффузионно-отражающих поверхностей). Даны различные аналитические методы, пригодные как для различного рода инженерных расчетов, так и для более детальных исследований. Особое внимание уделено аналитическому и численному исследованию лучистого обмена в цилиндрических и конических полостях и лучистому переносу через круглую трубу. Представлены результаты для различных видов отражательной способности поверхности. Вообще, найдено, что лучистый поток, исходящий из полости, увеличивается по мере того, как зеркальная компонента в отражательной способности поверхности растет. Аналогичное утверждение справедливо для случая передачи лучистой энергии через трубку.